

# Photoionization and photodissociation of furan by mass spectrometry and photoelectron imaging



Yihui Yan<sup>1, 2</sup> & Yuzhu Liu<sup>1</sup>

1 Nanjing University of Information Science & Technology, Nanjing, P. R. China

2 Chair of Physical Chemistry, Technical University of Munich, Germany

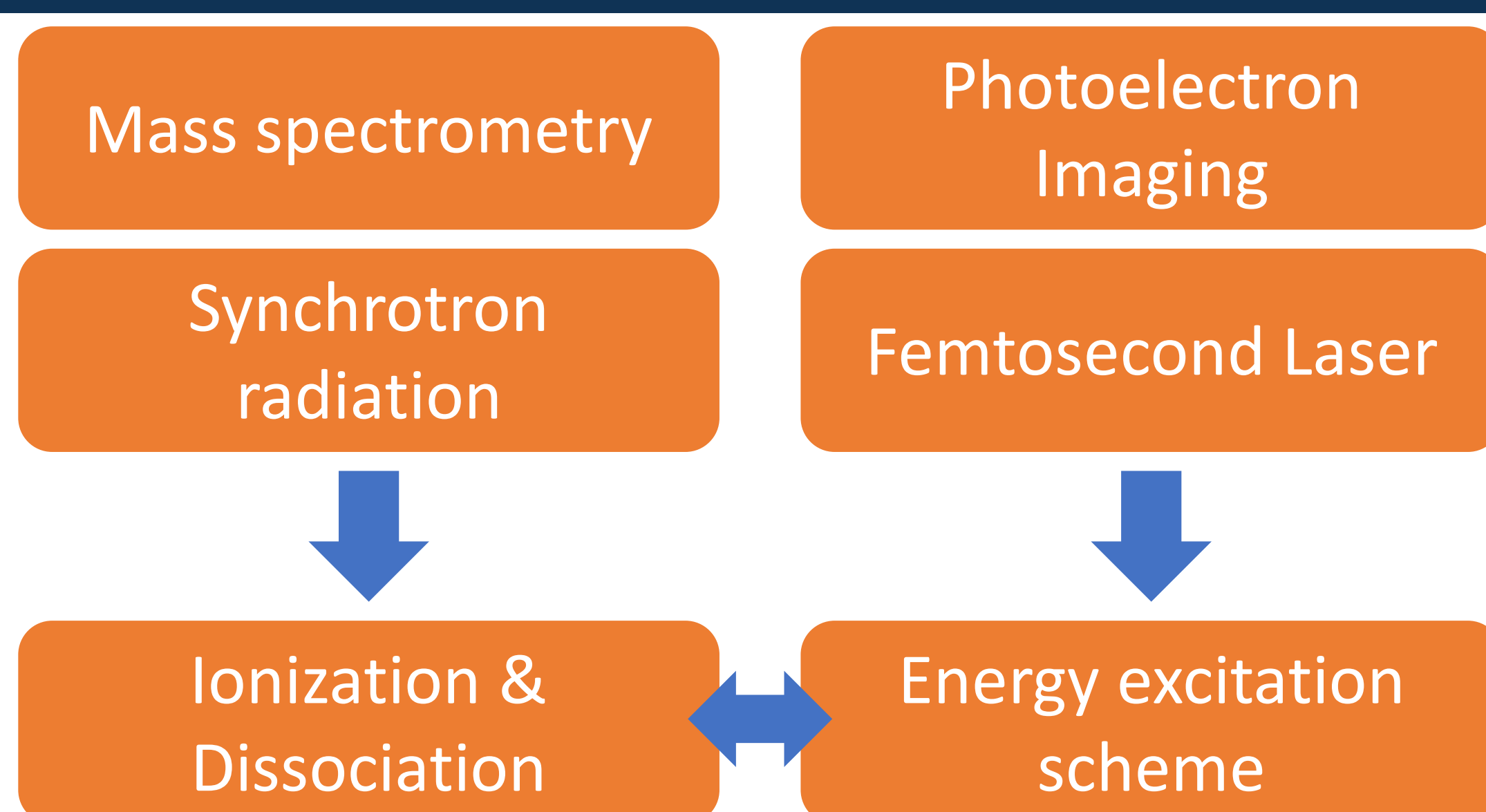
ISMB 2021

Email: yihui.yan@tum.de

Furan, a simple oxygen-containing aromatic molecule, undergoes a dissociation yielding two carbene intermediates. In order to clarify the exact decomposition pathways, we performed two distinct experiments. In the first one, a single photon absorption is used to probe the photoionization efficiency (PIE) of precursor and fragment ions by mass spectrometry and synchrotron radiation. The measured ionization potential of fragment ions such as  $C_4H_4O^+$  agrees with the theoretical value predicted by DFT. Based on the changes in PIE curves of fragment ions, we conclude that with the increase of energy,  $\beta$ -carbene will dominate, and  $C_3H_3^+$  becomes the main dissociation product.

The second one gives the energy scheme of furan at 400 nm femtosecond laser combined with photoelectron imaging. The ground and excited electronic states of furan are analyzed after four-photon absorption process and multiple energy bands were identified. Briefly, the energy band I relates to the ionization from the  $S_2$  state to the  $D_0$  state, and the appearance of the energy band II can be inferred to the rapid internal conversion from the  $S_2$  state to the  $S_1$  state after two-photon absorption. The energy bands III and IV are classified as the energy produced by the transition of the two filling states of the  $D_1$  state. At the same time, the energy bands V and VI are classified as the excitation energy of the two filled states, in which furan absorbs the four-photon transition to the  $D_0$  state.

## Methods



### Synchrotron Radiation

The energy range used in this experiment is 8.50 eV to 14.22 eV. Based on such an energy range, we choose argon as the filter gas to achieve the absorption of higher harmonics.

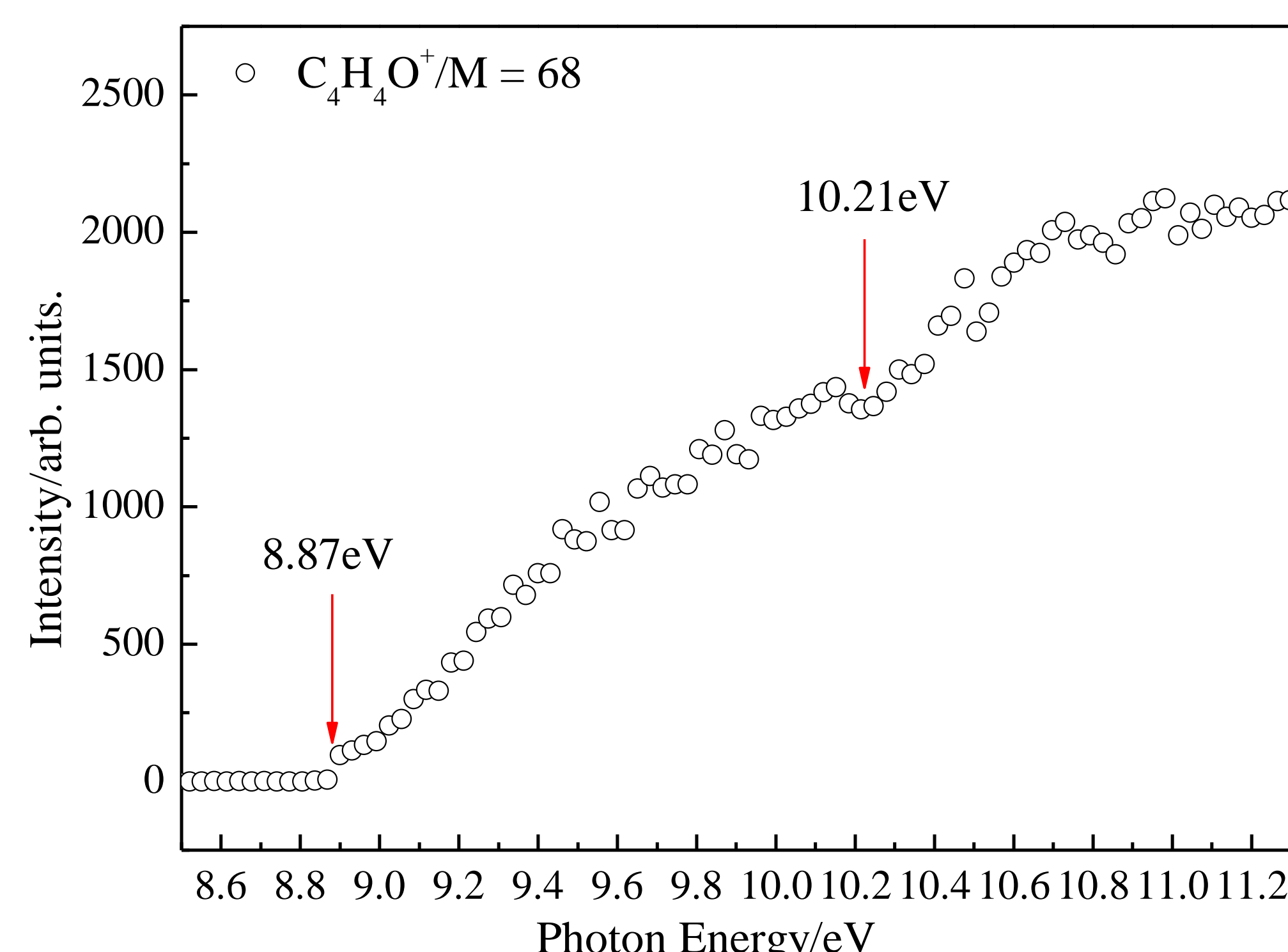
### Photoelectron imaging

The whole system includes two symmetrical and collinear 50 cm long no electric field flight tubes. Two time-of-flight mass spectrometers share the same light and matter interaction area. The three-dimensionally distributed charged particles are projected on the microchannel plate, and their flight time is obtained at the same time. The molecular beam was generated by injecting furan (Sigma-Aldrich, 99.0% purity) through a microvalve (Fa. Gyger) under a helium buffer (1.1 atm) at a pulse frequency of 400 Hz

## Ionization & Dissociation

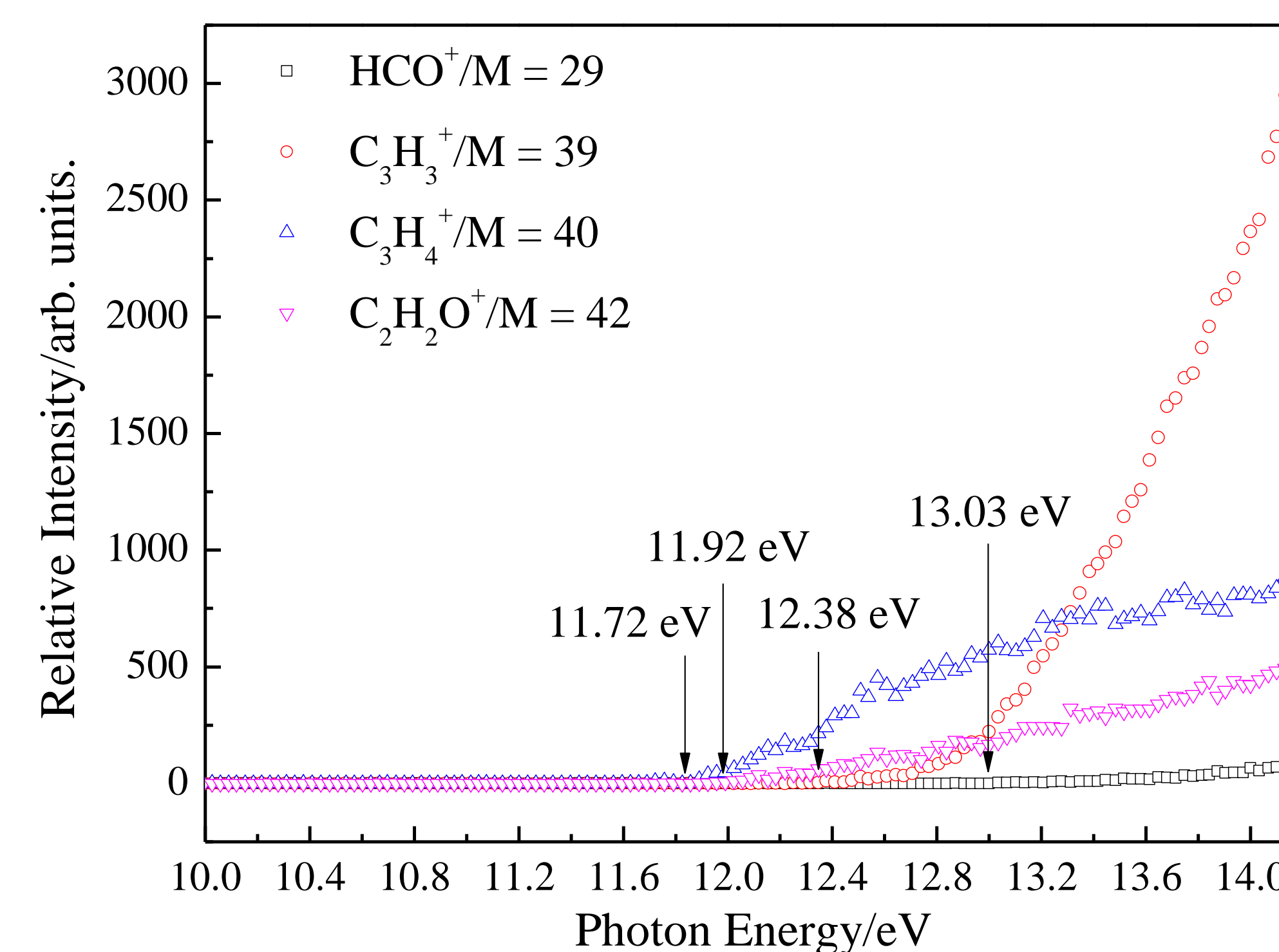
### Photoionization efficiency (PIE) curve of furan parent ion $C_4H_4O^+$

It can be found that the  $C_4H_4O^+$  was first obtained at 8.90 eV. The linear extrapolation method was used to calculate the appearance potential of furan parent ion as 8.87 eV, and the first ionization energy  $D_0$  was determined to be  $8.87 \pm 0.1$  eV. In addition, an inflection point falls into the plot of PIE curve as indicated by red arrow at 10.21 eV.



### Photoionization efficiency curve of $HCO^+$ , $C_3H_3^+$ , $C_3H_4^+$ and $C_2H_2O^+$ .

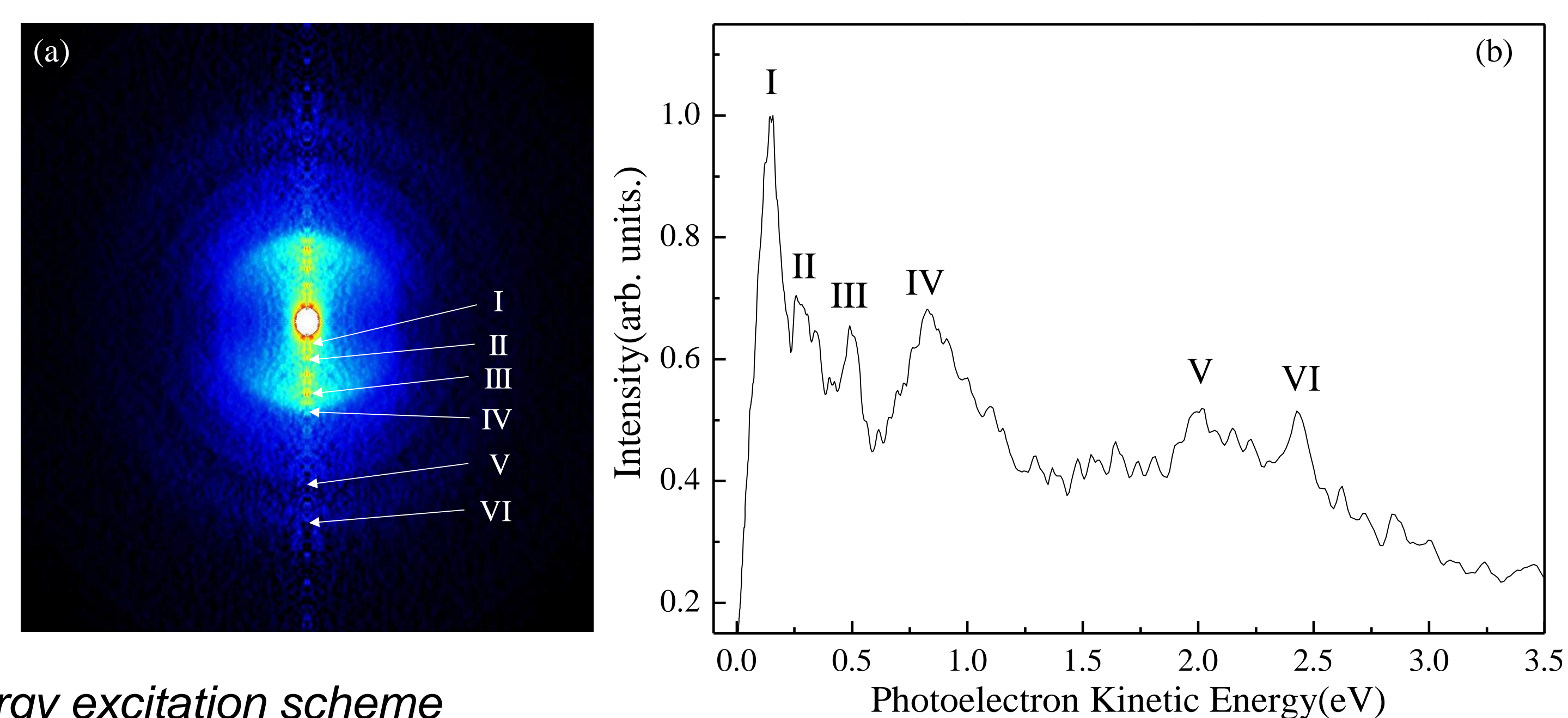
- When the SPE reached 11.72 eV,  $C_3H_4^+$  appeared first, resulting from the dissociation  $C_4H_4O^+ + h\nu \rightarrow C_3H_4^+ + CO$ .
- The dissociation channel corresponding to  $\alpha$ -carbene is  $C_4H_4O^+ + h\nu \rightarrow C_2H_2O^+ + C_2H_2$ , while the  $C_3H_4^+$  dissociation channel is  $\beta$ -carbene.
- The formation of  $HCO^+$  is the dissociation channel  $C_4H_4O^+ + h\nu \rightarrow C_3H_3 + HCO^+$ , and the emergence potential of  $HCO^+$  is 13.03 eV.
- When the SPE is greater than 12.93 eV, the  $\beta$ -carbene becomes the main dissociation channel contributing to  $C_3H_4^+$  and  $C_3H_3^+$ , and  $C_3H_4^+$  ions will also absorb some photons, forming a second photodissociation.
- $C_3H_3^+$  ions are obtained in two ways, one is parent ion dissociation, and the other is second photodissociation of  $C_3H_4^+$ .



## Energy excitation scheme

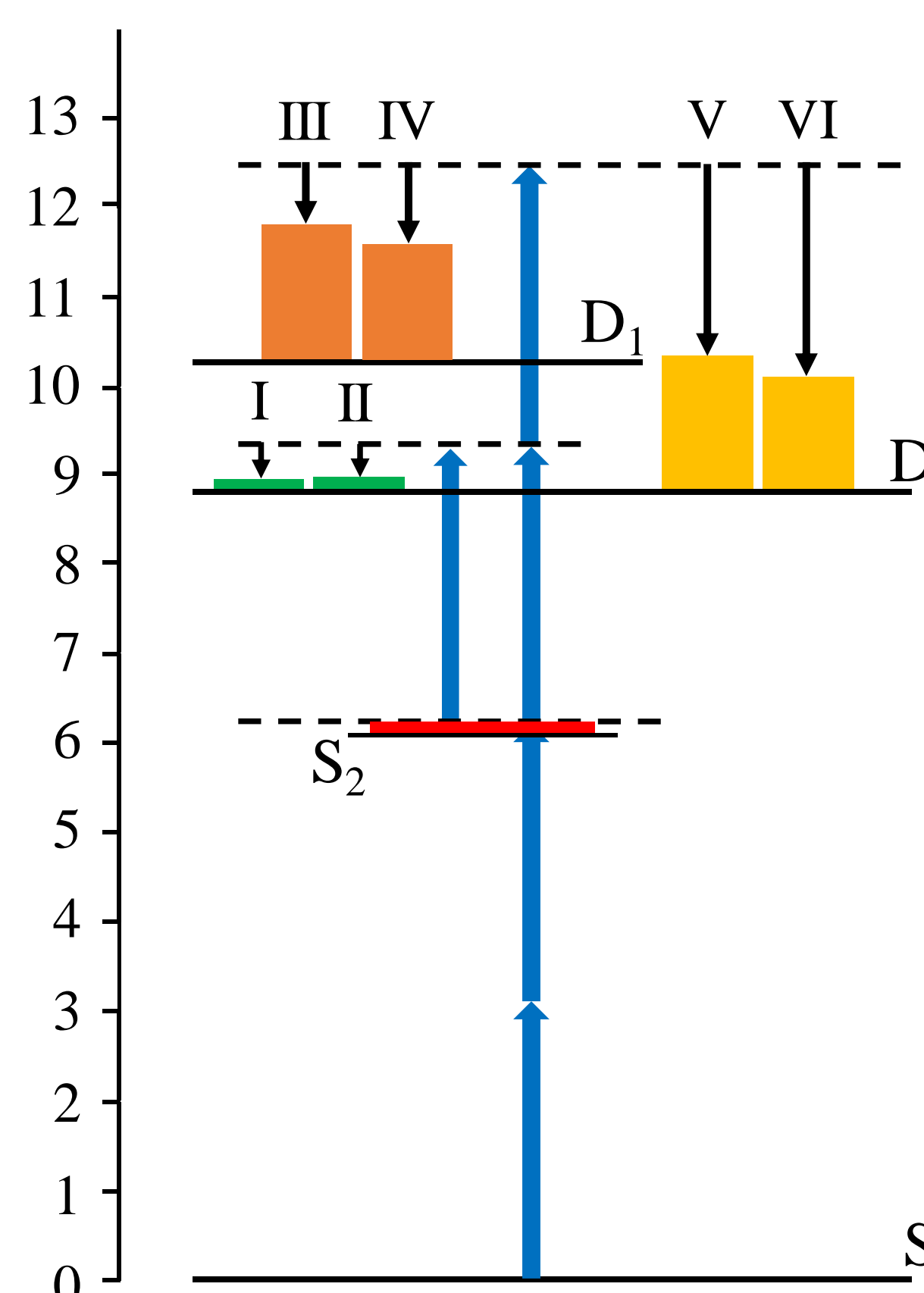
### Photoelectron image & furan photoelectron kinetic energy distribution

The linear polarization direction of the laser beam is perpendicular to the image, and the horizontal halo represents the momentum of the photoelectron. Five concentric photoelectron energy bands are distinguished, which are labeled as bands I, II, III, IV, V, and VI. An increase in the photoelectron energy band radius indicates an increase in kinetic energy. The distribution of photoelectron kinetic energy (PKE), the function of energy and delay time obtained by photoelectron imaging corresponds to the corresponding kinetic energy distribution. Therefore, the observed PKE curve is a function of the difference between the excitation energy in the relevant intermediate state and the energy of the finally reached state.



### Energy excitation scheme

The Figure shows the energy excitation scheme for furan to absorb 4 photons, including its ground state, excited state, and electronic state. The bands III, IV, V, VI with stronger kinetic energy can be inferred



as the energy that furan absorbs 4 photons (12.4eV) and ionizes into the  $D_0$  state and the  $D_1$  state. The position difference between band III and band V is  $\Delta_1 = 1.53$  eV, and the position difference between energy band IV and energy band VI is  $\Delta_2 = 1.59$  eV. The energy bands III and IV are classified as the energy produced by the transition of the two filling states of the  $D_1$  state. The energy bands V and VI are classified as the excitation energy of the two filled states in which furan absorbs the 4-photon transition to the  $D_0$  state. Both  $\Delta_1$  and  $\Delta_2$  are close to the energy level difference between the  $D_0$  state and the  $D_1$  state, and this type of distribution can be confirmed.

## Acknowledgment

This work was supported by National Natural Science Foundation of China (Grant No. U1932149), Natural Science Foundation of Jiangsu Province (Grant No. BK20191395). We gratefully acknowledge the assistance of Jozef Lengyel.

## Reference

- [1] K. N. Urness, et al. Journal of Chemical Physics. 139, 124305 (2013).
- [2] Y. Yan, et al. Chemical Physics. 530, 110611 (2020)
- [3] Y. Liu, et al. Chemical Physics. 446, 142-147 (2015)